

STRAIN ANALYSIS OF BONE HEALING

K. Řehák^{*}, B. Skallerud^{**}

Abstract: *The distraction osteogenesis has an important position in orthopedic surgery, and it is still object of research to get better understanding of bone healing. The response of callus bone to mechanical loading can be used for assessment of treatment progress. The mechanical strain distribution is often used for assessment in case of bone remodeling (Frost, 1994), thus it could provide additional information of fracture healing progress as well. The strength of the whole callus bone is significantly affected by architecture and tissue properties, which are very difficult to obtain. This article presents finite element analysis of bone fracture healing based on input information obtained from micro-CT scans. The objective of this study is to find which part of callus determines the maximal appropriate loading of whole callus. The four pieces of rabbit tibia fracture callus were micro-CT scanned 30 days after osteotomy using an isotropic voxel size of 20 μm . All finite element models were axially loaded to investigate the reaction force value for different segments of the callus. The mechanical strain distribution and reaction forces of callus were evaluated to compare the differences between each part of models. The results show that the present approach by using finite element method (FEM) is a useful tool in understanding and assessment of fracture healing process.*

Keywords: Micro-CT, Fracture callus, Microstructure, Tissue properties, Finite element method.

1. Introduction

Many people suffer from unequal length of extremities or dwarfism. One treatment procedure is offered in orthopaedics by means of distraction osteogenesis (bone lengthening). The whole process of distraction osteogenesis could be separated into two phases, bone lengthening and consolidation (fixed length, bone maturation). In this second phase of fracture healing, the callus consists of several tissue types. The bone reacts to the mechanical loading by remodeling if it is loaded optimally. The mechanostat hypothesis describes the process of how bone responds to loading (Frost, 1994). This approach can be used for bone healing process at the end of the second phase of bone lengthening.

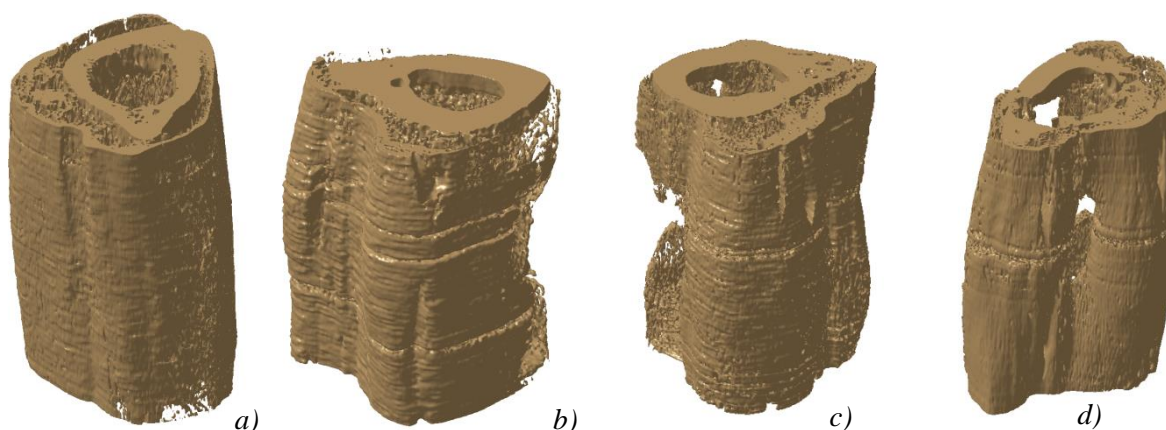


Fig. 1: Shape of all callus a), b), c), d).

^{*} Ing. Kamil Řehák: Brno University of Technology, Faculty of Mechanical Engineering, Institute of Solid Mechanics, Mechatronics and Biomechanics, Technická 2896/2, 616 69 Brno, CZ, kamil.rehak@gmail.com

^{**} Prof. dr. Ing. Bjorn Helge Skallerud: Norwegian University of Science and Technology, Department of Structural Engineering, Richard Birkelands vei 1a, 7491 Trondheim, Norway, bjorn.skallerud@ntnu.no

This study of callus bone response was performed on four rabbit tibia subjected to mid-diaphyseal osteotomy and distraction osteogenesis. The geometry of all callus is shown in Fig. 1. After 30 days (10 days distraction and 20 days consolidation) each callus was scanned using a high resolution micro-CT system [SCANCO Medical AG]. The length of each callus was in range of 10-12 mm, the cross-section diameter is approximately 8 mm. The specimen was scanned at 20 μm resolution. More details can be found in (Aleksyniene et al., 2009).

If a voxel based finite element mesh of the whole rabbit callus is created, using the 20 micrometer scanning resolution, one ends up with approximately 150 million finite elements. This is not computationally feasible without supercomputers and parallelized numerical schemes, thus some simplifications are necessary.

The overall goal of this study was to determine which part of the callus provides the most important stiffness. The FEM software ANSYS was used for this purpose. The detailed finite element models are created from microCT files (Marcian et al., 2012; Marcian et al., 2012).

2. Methods

The scans obtained from micro-CT were segmented in STL Model Creator (Marcian et al., 2011), where saving of pixel intensities is enabled. The pixel intensity can be recalculated to Young's modulus, thus the material properties can be read into finite element software according to element position (Fujiki et al., 2013; Valasek et al., 2010). The dependence of pixel intensity in microCT scans and Young's modulus value is shown in Fig. 2, which is similar to other work (Fujiki et al., 2013; Shefelbine et al., 2005). The range of pixel intensity is 0-4095. The maximum value of Young's modulus was determined based on La Russa (2012), where experiments and numerical models were compared in three point bending. The computational model of each callus is created accounting only for voxels with pixel intensity above 1250. The computational model of callus A with nonhomogeneous linear elastic material properties is shown in Fig. 3. In order to have feasible FE models, instead of using solid elements with 20 micrometer edge, the size was set to 60 micrometer. This led up to 4 millions elements for each segment of callus. The discretization was created using the tetrahedral 10-node element SOLID187, which has a quadratic displacement interpolation and is convenient in capturing details and avoiding bad element shapes. Each callus was divided into five segments. Each segment was axially loaded by 0.1% elongation by prescribing displacement at the bounding sections of the segment. Afterwards the corresponding reaction force was calculated. This provides information about how the stiffness is distributed along the callus.

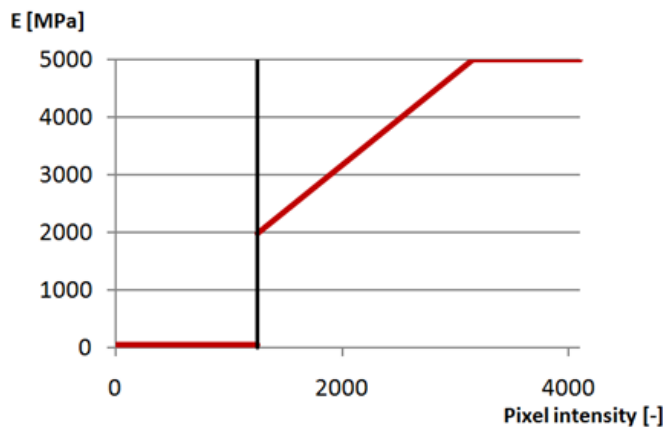


Fig. 2: Young's modulus dependence on pixel intensity.

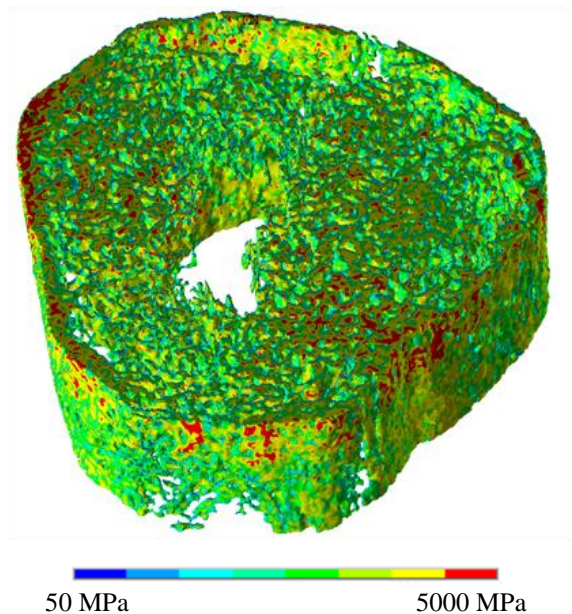


Fig. 3: Young's modulus of callus A second segment.

3. Results

The reaction force due to the displacement loading was calculated for each segment and compared to the highest value of each callus. The distribution of the reaction force along callus is shown in Fig. 4. The highest value of force, which corresponds to 0.1% segment strain, is dominantly in middle segment in case of callus B, C, D; and in the second segment in callus A. On the other hand the force difference between second and third segment of callus A is not so significant. The lowest value of force is 46%, but the reaction force of third segment of callus D is significantly higher than in other segments. The highest value in the middle part could be due to the callus cross section, which is largest in the middle part of the callus and smaller at the ends. Also the material properties are important in this regard. The quantity of mineralized tissue is significantly changing through whole process of healing (Morgan et al., 2009). The time of scanning callus corresponds to end of second phase (consolidation). At the callus ends the old cortical bone is present and new bone must be connected to them, which is more difficult than creation of new bone in the whole volume, like in the middle.

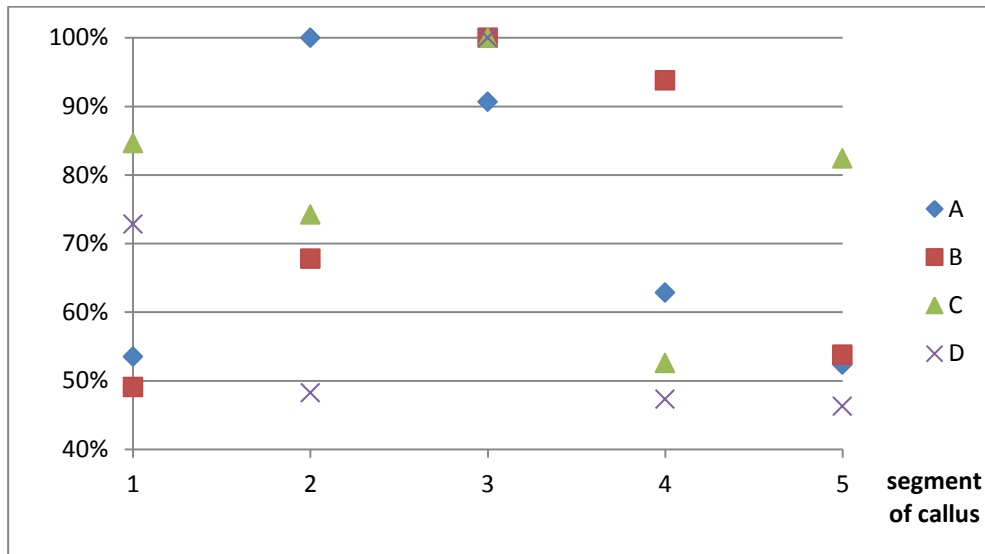


Fig. 4: Reaction force due to 0.1% nominal strain in percent of highest value of each callus.

The mechanical strain distribution of four calluses was investigated to see if the response to mechanical loading is physiological or pathological overloading. In the present study we use microstrain to assess callus model response. A closer study of strain distributions shows that the whole callus is in physiological loading, thus the remodelling of callus can be expected. Physiological loading is defined for strain 0.0002-0.002. (Frost, 1994) The strain distribution of callus A is shown in Fig. 5.

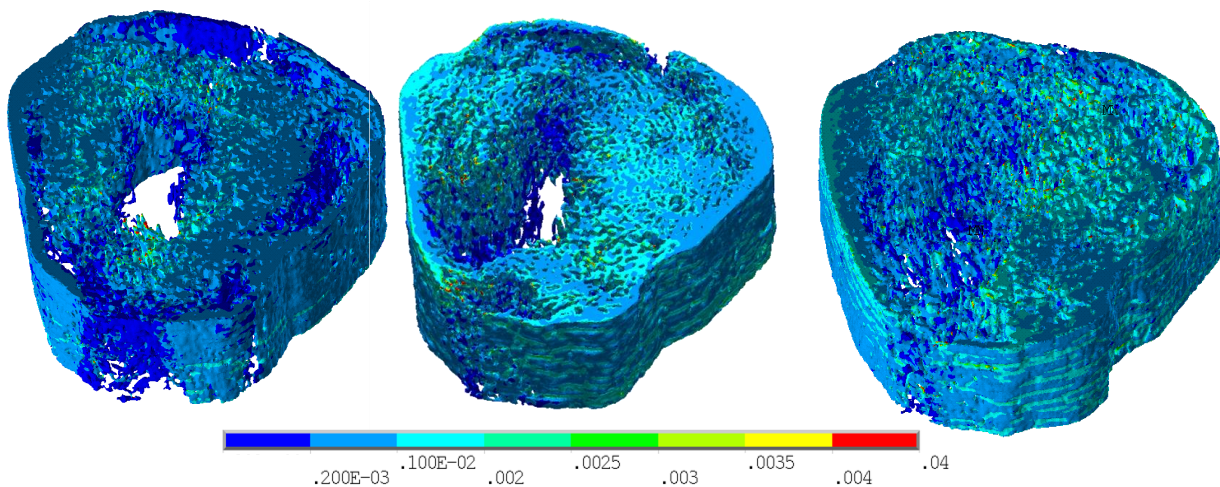


Fig. 5: Strain distribution of callus A, first, second and third part.

4. Conclusions

The present study focused on determination of which part of callus has lower stiffness and governs the optimal loading to support bone healing. To find the lowest stiffness part the four calluses were divided into five parts, which were loaded by elongation 0.1%. The reaction forces were evaluated and compared to the highest value of each callus. The analysis of the callus shows that the end parts were the low stiffness segment, thus the optimal loading should be determined based on them. The middle part seems to be stiffer due to larger cross-section, moreover the material properties of this part at this healing phase are getting closer to mature bone mechanical properties.

The results of finite element analysis show that the callus reaction to loading can be evaluated by mechanical strain distribution, which is dominantly below the bone pathological overloading value.

Further work should deal with better determination of critical callus location, and time dependent analysis is necessary to perform (Vetter et al., 2011). The micro-CT should be done through whole phase of healing and the new experiments should be done to get more accurate estimates of Young's modulus.

Acknowledgement

This work was supported by specific research FSI-J-12-5 and specific research FSI-S-14-2344. The authors are grateful for input from Drs. R. Aleksyniene and V. Russa.

References

- Aleksyniene, R., Thomsen, J. S., Eckhardt, H., Bundgaard, K. G., Lind, M., Hvid, I. (2009) Three-dimensional microstructural properties of regenerated mineralizing tissue after OTH treatment in a rabbit tibial lengthening model, *J Musculoskelet. Neuronal Interact.* 9, pp. 268-277.
- Frost, H. M. (1994) Wolff's law and bone's structural adaptations to mechanical usage: an overview for clinicians, *The Angle Orthodontist*, Vol. 64, No. 3, pp 175-188.
- Fujiki, K., Aoki, K., Marcian, P., Borák, L., Hudieb, M., Ohya, K., Igarashi, Y., Wakabayashi, N. (2013) The influence of mechanical stimulation on osteoclast localization in the mouse maxilla: bone histomorphometry and finite element analysis, *Biomech and Mod in Mechanobio*, pp. 325-333.
- LaRussa, V. (2012) Biomechanical aspects of distraction osteogenesis, PhD Thesis, Dep Structural Engineering, Norwegian Univ Science and Techn.
- Marcian, P., Konecny, O., Borak, L., Valasek, J., Rehak, K., Krpalek, D., Florian, Z. (2011) On the Level of Computational Models in Biomechanics Depending on Gained Data from CT/MRI and Micro-CT, *Mendel*, pp. 255-267.
- Marcian, P., Majer, Z., Dlouhy, I., Florian Z. (2012) Estimation of Local Mechanical Properties of Highly Porous Ceramic Materials, *Chemicke listy*, pp. 476-477.
- Marcian, P., Majer, Z., Florian Z., Dlouhy, I. (2012) Stress Strain Analysis of High Porous Ceramics, *Advanced Materials Research*, pp. 1330-1333.
- Morgan, E. F., Mason, Z. D., Chien, K. B., Pfeiffer, A. J., Barners, G.L., Einhorn, T. A., Gerstenfeld, L. C. (2009) Micro-computed tomography assessment of fracture healing: Relationships among callus structure, composition and mechanical function, *Bone* 44, pp. 335-344.
- Shelfelbine, S. J., Simon, U., Claes, L., Gold, A., Gabet, Y., Bab, I., Muller, R., Augat, P., (2005) Prediction of fracture callus mechanical properties using micro-CT images and voxel-based finite element analysis, *Bone* 36 480-488.
- Valasek, J., Marcian, P., Krpalek, D., Borak, L., Florian, Z., Konecny, O. (2010) Material Properties of Bone Tissue Obtained from CT for Biomechanics Purposes, *Mendel Journal series*, pp. 483-490.
- Vetter, A., Liu, Y., Witt, F., Manjubala, I., Sander, O., Epari, D.R., Fratzl, P., Duda, G.N., Weinkamer, R. (2011) The mechanical heterogeneity of hard callus influences local tissue strains during bone healing: A finite element study based on sheep experiments, *Journal of Biomechanics* 44, pp 517-523.